Vietnam Journal of Mechanics, Vol. 45, No. 3 (2023), pp. 247 – 258
DOI: https://doi.org/10.15625/0866-7136/19024

DESIGN, MODELING, AND EXPERIMENTAL EVALUATION OF A SELF-SEALING COMPONENT FOR ROTARY SHAFTS IN MAGNETO-RHEOLOGICAL FLUID DEVICES

Vo Van Cuong[1], Quoc Hung Nguyen[2,*], Le Hai Zy Zy[1], Ngoc Diep Nguyen[1], Le Duy Tuan[1], Do Huu Minh Hieu[2], Do Quy Duyen[2]

[1]*Department of Mechanical Engineering, Industrial University of Ho Chi Minh City, Ho Chi Minh City, Vietnam*

[2]*Faculty of Engineering, Vietnamese-German University, Binh Duong, Vietnam*

[*]E-mail: hung.nq@vgu.edu.vn

Received: 11 September 2023 / Published online: 30 September 2023

Abstract. This study focuses on the development and evaluation of a self-sealing component for rotary shafts in Magneto-rheological (MR) fluid-based devices, such as MR brakes and MR clutches. The proposed sealing component, which replaces traditional lip-seals, consists of a permanent magnet and a magnetic core positioned on the rotary shaft. Through a combination of simulation and experimentation, the design and performance of the self-sealing component are investigated. Initially, the research provides an overview of MR fluid and its applications, as well as previous studies on sealing components utilizing MR fluid. Building on this background, a configuration for the self-sealing component specific to rotary shafts in MR fluid-based devices is proposed. The design and modeling of the sealing component are carried out, employing the Bingham plastic rheological model of the MR fluid and finite element analysis techniques. Through finite element analysis, an optimal design for the sealing component is determined. Prototypes of the sealing component are manufactured, and experimental testing is conducted to assess its performance characteristics. The experimental results are then compared with the simulated results, allowing for a comprehensive evaluation of the sealing component's effectiveness.

Keywords: magnetorheological fluid (MRF), MRF seal, optimal design, permanent magnet.

1. INTRODUCTION

In recent years, extensive research has been conducted on the utilization of magnetorheological fluid (MRF) in various applications, including MR dampers, MR brakes and

clutches, MR engine mounts, MR valves, and more [1]. While there have been some studies on employing MRF in sealing to prevent fluid leakage, these investigations have been limited and primarily focused on specific cases [2–5]. Furthermore, prior research has not adequately addressed the calculation, optimal design, and experimental verification of fundamental features of seal-based devices, such as frictional torque, heat generation, and life cycle, nor have they provided comparisons with traditional seals. For example, Kordonski et al. [1] conducted experiments to assess the effectiveness of seals utilizing MRF in preventing air leakage through shaft gaps in pressurized chambers. Their results showed variations in the maximum working pressure without leakage for different strengths of excited magnetic fields. Additionally, the friction torque generated by the MR fluid was found to be minimal, which is advantageous for sealing applications. Similarly, Matuszewski et al. [2] proposed several MRF seal configurations for underwater equipment but did not perform modeling, calculations, or experiments. Urreta et al. [3] explored the use of MRF for sealing rotating shafts in precision machines and found that the frictional torque was negligible, with variations observed when different MR fluids were employed. Hegger et al. [4] introduced a smart seal configuration to prevent MRF leakage in an MR actuator, reporting minimal frictional torque and system durability for up to 6 months. Kubík et al. [5] conducted experiments demonstrating the prevention of MRF leakage using magnetic fields, resulting in significantly low frictional torque.

In this study, we focus on developing new configurations, optimal designs, and experimentally validating sealing devices that utilize MRF, referred to as MRF seals. Specifically, the seals are designed for cases where MRF serves as the working fluid, such as in MR clutches, MR brakes, and MR actuators. The subsequent section presents the configuration of the proposed MRF seal, followed by modeling based on the Bingham plastic rheological model of the MR fluid and finite element analysis. Through finite element analysis, an optimal solution for the MRF seal is obtained. Prototypes of the optimized MRF seal are fabricated, and experimental testing is conducted to evaluate its performance characteristics. The experimental results are then compared with simulated outcomes, providing a comprehensive assessment of the MRF seal's effectiveness.

2. CONCEPTUAL DESIGN OF THE MRF SELF SEALING COMPONENT

Fig. 1 illustrates the proposed configuration of the MRF seal, featuring rectangular-shaped poles. The diagram also highlights the significant geometric dimensions associated with the seal. The MRF seal comprises various components, including a permanently magnetized magnet, magnetic poles, a magnetic sleeve (utilized when the shaft is nonmagnetic), a nonmagnetic separator, and a nonmagnetic housing. The permanent magnet, affixed to the two poles, plays a crucial role in the MRF seal by generating a magnetic field with flux passing through the MRF at the poles, effectively preventing leakage

of the MR fluid. Various magnet shapes, such as blocks, rings, cylinders, radial assemblies, and Halbach assemblies, can be implemented. For simplicity and cost-effectiveness, this study employs an axially magnetized ring-shaped magnet. The nonmagnetic separator is employed to prevent magnetic flux from passing directly from one pole to the other without crossing the MRF gap, while also ensuring no contact occurs between the MRF and the magnet. The nonmagnetic housing, composed of nonmagnetic material, safeguards against magnetic field loss to the surroundings. With the presence of magnetic field across the MRF gap, magnetic particles within the fluid are attracted to one another, aligning themselves along the magnetic flux lines. Consequently, the MRF exhibits a nearly solidified behavior. This phenomenon effectively aids in preventing MRF leakage, enhancing the sealing capability of the system.

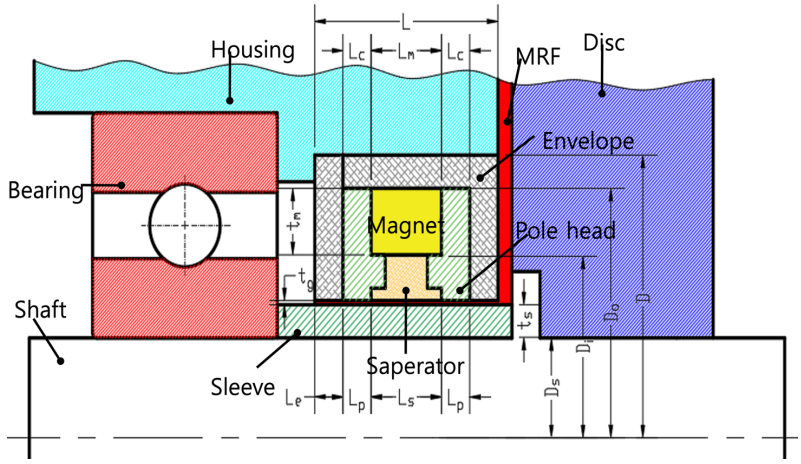

Fig. 1. Configuration of the MRF self sealing component

3. MAXIMUM WORKING PRESSURE AND FRICTIONAL TORQUE OF RF-SEALING COMPONENT

The maximum working pressure of the MRF seal is defined as the pressure at which the MRF flow initiates within the MRF gap. In this analysis, it is assumed that the pressure at the exit of the MRF seal is equal to atmospheric pressure. Therefore, the maximum working pressure of the seal corresponds to the pressure drop experienced by the MRF flow as it passes through the seal gap. During the initial phase of MRF flow, the velocity within the gap is negligible, approaching zero. As a result, the pressure drop attributed to the viscosity of the MRF can be disregarded. Consequently, the pressure drop associated with the MRF flow through the MRF gap, representing the maximum working pressure of the seal, can be determined using the following relation [6]:

$$P_{\max} = \Delta P = c_1 \frac{L_{p1}}{t_g}\tau_{y1} + c_2 \frac{L_{p2}}{t_g}\tau_{y2} + c_3 \frac{L_{p3}}{t_g}\tau_{y3} + 2c_4 \frac{L_e}{t_g}\tau_{y4}. \quad (1)$$

In the given equation, L_{p1} represents the length of the inner pole, while L_{p2} corresponds to the length of the outer pole. Additionally, L_{p3} denotes the length of the MRF duct at the nonmagnetic separator, and L_e represents the envelope length. The coefficients c_1, c_2, c_3 and are factors that depend on the velocity profile of the MRF flow within the gap. Due to the significantly low velocity of the MRF flow, these coefficients are approximately equal to 2.0.

In this investigation, the induced yield stress (τ_y) of the MRF is modeled as a function of the induced magnetic flux intensity across the MRF gap. The relationship between τ_y and the magnetic flux intensity is determined through experimental curve fitting, as outlined in previous research [7].

$$\tau_y = 2.717 \times 10^5 C\Phi^{1.5239} \tanh(6.33 \times 10^6 H). \quad (2)$$

In the given relationship, τ_y represents the induced yield stress in pascals (Pa), while Φ and H (A/m) denote the volume fraction of iron in the MRF and the applied magnetic flux intensity through the MRF clearance, respectively. It should be noted that the coefficient C is influenced by the carrier fluid, such as hydrocarbon oil having a value of C = 1.0, water with C = 1.16, and silicone oil with C = 0.95.

The viscosity of the Magnetorheological Fluid (MRF) is considered to be unaffected by the applied magnetic field. Eq. (3) is an empirical equation utilized to describe the viscosity of the MRF based on the working temperature.

$$\eta = \eta_{40} \exp\left[\frac{(1 + 2.43\Phi)(40 - T)}{48 - T}\right]. \quad (3)$$

In this equation, denoted by symbols, we have η representing the viscosity at the operational temperature in Pascal, η_{40} as the viscosity of the MRF at 40 °C, Φ indicating the volume fraction of iron in the MRF as a percentage, and T representing the operational temperature of the MRF in degrees Celsius.

The friction torque of the MRF seal is determined as the torque resulting from the MRF's friction within the gap and its effect on the shaft. This friction torque can be computed using the formula provided in reference [8].

$$T_f = T_{f1} + T_{f2} + T_{f3} + 2T_{f4}. \quad (4)$$

The frictional torque of the MRF at the inner pole, separator, and outer pole, denoted T_{f1}, T_{f2}, T_{f3} as respectively, can be determined using the following equations

$$T_{f1} = 2\pi R_s^2 L_{p1}\left(\tau_{y1} + \eta\frac{\Omega R_s}{t_g}\right), \quad (5)$$

$$T_{f2} = 2\pi R_s^2 L_{p2} \left(\tau_{y2} + \eta \frac{\Omega R_s}{t_g} \right), \tag{6}$$

$$T_{f3} = 2\pi R_s^2 L_{p3} \left(\tau_{y3} + \eta \frac{\Omega R_s}{t_g} \right), \tag{7}$$

$$T_{f4} = 2\pi R_s^2 L_e \left(\tau_{y4} + \eta \frac{\Omega R_s}{t_g} \right). \tag{8}$$

Here, the variables used in the equation are as follows: R_s is the shaft radius and $\tau_{y1}, \tau_{y2}, \tau_{y3}, \tau_{y4}$ are respectively yield stress of the MRF in $L_{p1}, L_{p2}, L_{p3}, L_{p4}$. η is the post-yield viscosity of MRF, Ω is the velocity of the shaft which is measured in rounds per minute, t_g is the MRF gap.

4. OPTIMAL DESIGN OF THE MRF SEAL

The design of MRF-based seals involves several crucial factors, including the maximum working pressure, overall length, and diameter. These parameters play a significant role in replacing conventional seals or ensuring interchangeability. The objective of the research is to maximize the working pressure while ensuring that the dimensions, such as length and diameter, do not exceed the required values. Mathematically, the optimal design problem for the MRF-based seal can be defined as follows: Determine the optimal values for key geometric dimensions, including pole length (L_{p1}, L_{p2}), permanent magnet size (L_m, D_i, D_o), sleeve thickness (t_s), envelope length (L_e), and core length (L_{c1}, L_{c2}), in order to maximize the working pressure as defined by Eq. (1). This optimization is subject to the constraints: $L \leq L_{sl}$; $D \leq D_{sl}$, where D_{sl} and L_{sl} represent the diameter and length of the constrained volume determined by the overall size of the equivalent lip seal.

It is worth noting that a smaller MRF gap size leads to higher pressure drop but also results in increased frictional torque. Additionally, manufacturing benefits and potential wear issues should be taken into account. For this study, the MRF gap size is empirically set at 0.2 mm. The seal structure is assumed to be symmetric, meaning that ($L_{p1} = L_{p2}$) and ($L_{c1} = L_{c2}$). To solve the optimization problem, a first-order optimization method with a gradient descent algorithm integrated into the ANSYS software's optimization toolbox is utilized. The optimization procedure can be outlined as follows: The magnetic circuit problem of the MRF seal is addressed by employing the APDL language with arbitrary initial values assigned to the design variables. To determine the average magnetic intensity across the three sections of the MRF gap, a path operation is employed. A path is defined along the gap, and the magnetic intensity across the MRF gap is mapped onto this path. The average magnetic intensity is then evaluated by integrating the intensity

along the path. The induced yield stress within the sections of the MRF gap and the post-yield viscosity of the MRF are calculated using Eqs. (2) and (3) respectively. Subsequently, the maximum working pressure and the frictional torque are computed using Eqs. (1) and (4) respectively. It is noted that the magnetic property of the MRF is expressed by B-H curve which is approximately determined by the following equation [7].

$$B = 1.91\Phi^{1.133}\left[1 - \exp(-10.97\mu_0 H) + \mu_0 H\right]. \tag{9}$$

In the above equation, B is the flux magnetic density (Tesla), H is the exerted magnetic flux intensity (A/m), $\mu_0 = 4\pi.10^{-7}$ Tm/A is the permeability of vacuum and Φ is volume fraction of the MRF.

5. RESULTS AND DISCUSSIONS

In this section, the optimal results of the MRF seals are obtained, and detailed discussions are presented. The magnetic components such as the housing, sleeve, two magnetic cores, and poles are made of commercial steel S45C. The MRF used in this study is MRF132-DG produced by LORD Corporation. The nonmagnetic parts, including the envelope and separator, are made of stainless steel. The commercial magnets are utilized with the following specifications: The magnet material is NdFeB (Neodymium Iron Boron), specifically Grade N42, the magnetization direction is axial, the pull force of the magnet is approximately 2.60–2.90 lbs, the maximum values for the remanent magnetic induction (Brmax) and the maximum energy product (Bhmax) are 13,200 gauss and 42 MGOe (Mega-Gauss Oersted), respectively.

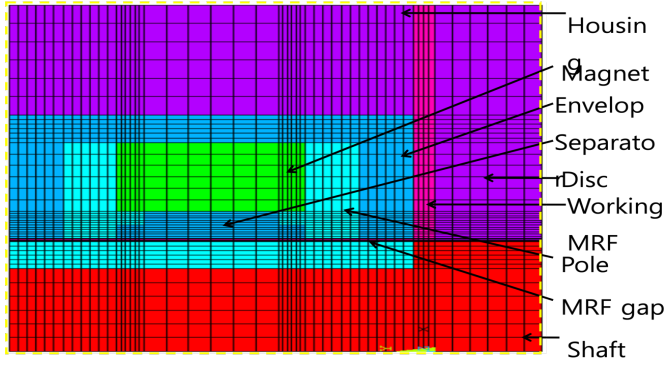

Fig. 2. Finite element model for magnetic analysis of the MRF seal

Fig. 3 illustrates the optimal solution of the MRF seal within the constrained working space defined by D_{sl} = 30 mm, L_{sl} = 10 mm, and D_s = 10 mm. These constraints are determined based on the overall size of the commercial lip-seal Parker-62576. The convergence rate of the optimization is set at 0.1%. As shown in Fig. 3(a), convergence is

achieved at the 25th iteration, resulting in a maximum working pressure of 26.18 bar, an overall length of 10 mm, and an outer radius of 30 mm (as constrained). The design variables of the optimal solution are presented in Fig. 3(b). Table 1 summarizes the optimal solution at the 25th iteration.

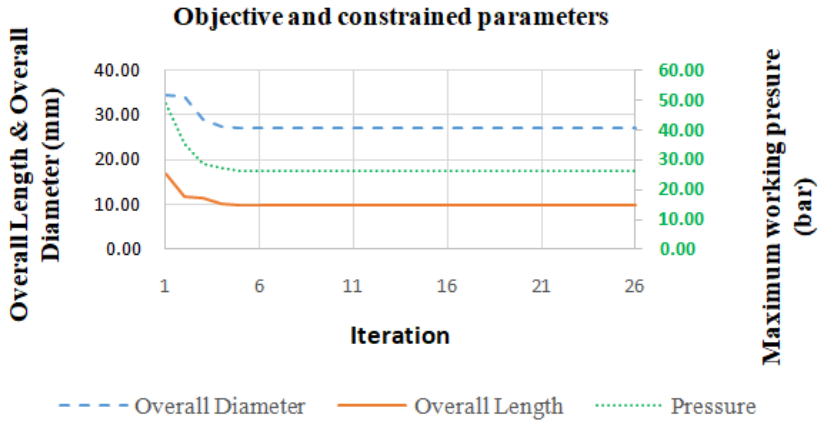

(a) Objective and constraints

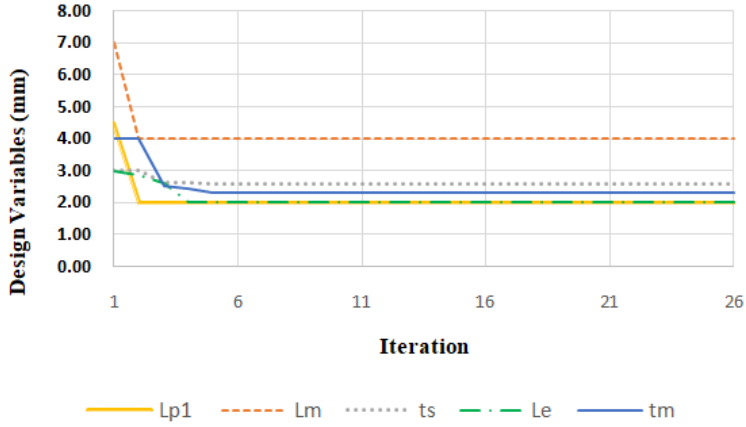

(b) Design variables

Fig. 3. Optimal solution of the MRF seal using ANSYS

Fig. 4 displays the magnetic density distribution of the MRF seal at the optimum. It is worth noting that based on the optimal results and considering the availability of commercial magnets, the actual sizes of the magnet are as follows: L_m = 2 mm, D_i = 18 mm, D_o = 25 mm.

Table 1. Optimal results of the MRF seal

Parameters	Characteristics
Overall Length: L = 10 mm Overall diameter: D = 27.32 mm Inner diameter of the magnet: D_i = 18.62 mm Outer diameter of the magnet: D_o = 23.32 mm Outer diameter of the sleeve: D_g = 15.22 mm Pole length: $L_{p1} = L_{p2}$ = 1.5 mm Magnet length: L_m = 3.5 mm Separator length: L_{p3} = 3.5 mm The enveloped thickness: L_e = 1.5 mm The magnet thickness: t_m = 2.35 mm	Max. Pressure: ΔP = 26.18 bar Frictional torque: T_f = 0.037 Nm

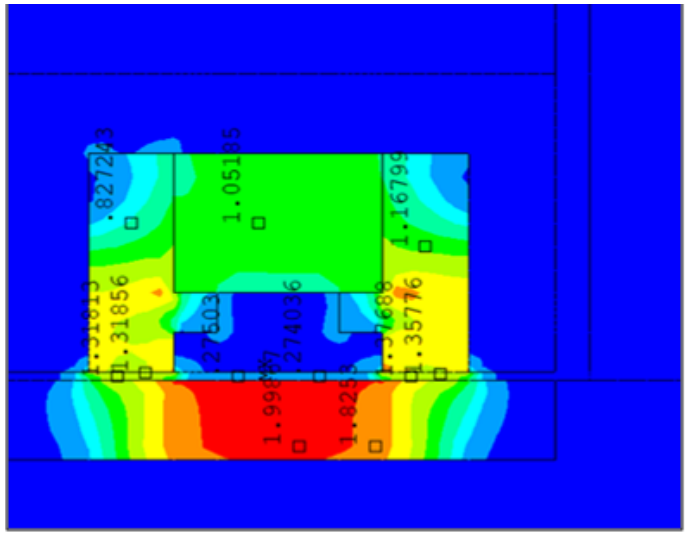

Fig. 4. Distribution of magnetic density of the optimized MRF seal

6. CONCLUSIONS

Fig. 5 illustrates the experimental setup used to test the performance of the MRF seal including torque measurement and observation of potential MRF leakage. The setup includes the following components and features: A servo motor is employed to drive the shaft of the MRF device. The motor provides rotational motion to the system, a disc is attached to the shaft of the MRF device. The motion of the servo motor is transferred to the disc, causing it to rotate, the space between the disc and the fixed housing forms a chamber. This chamber is filled with MRF and can be pressurized using a piston-cylinder system connected to the pressure control port. The pressure applied to the MRF can be

controlled in this setup, two MRF seals are installed on both sides of the shaft to prevent MRF leakage from the chamber to the bearings or other parts of the setup, to observe any potential leaking of the MRF, a slot is machined on the housing. This allows visual inspection of the MRF and detection of any leakage. The housing of the MRF device is fastened to the motor support on one end and fixed to the middle support on the other end. It provides structural support and stability to the system. The output shaft of the MRF device is connected to the torque sensor shaft through a mechanical coupling. The torque sensor measures the torque applied to the system and provides a corresponding signal. The measured signal from the torque sensor is transmitted to the computer through the torque transducer. This allows the evaluation and analysis of the torque measurements. The speed of the servo motor can be controlled by a computer through the motor drive. The computer also receives and processes the measured torque signal for further analysis and evaluation.

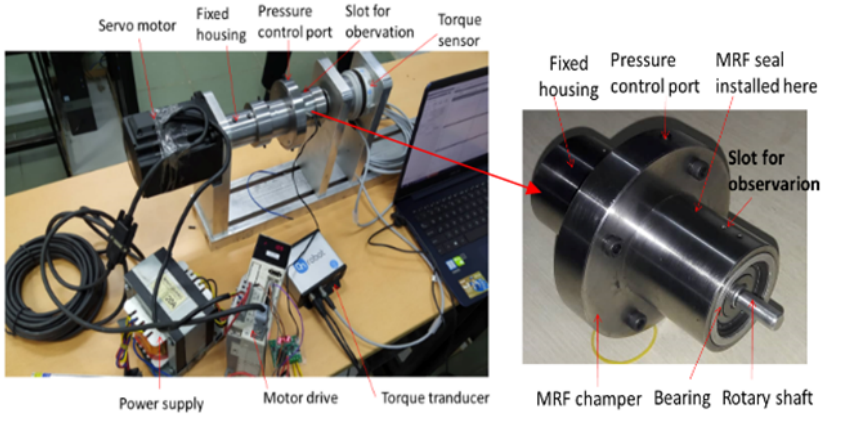

Fig. 5. Experimental setup for MRF seal testing

In the first experiment, the frictional torque of the MRF seal and the lip-seal are measured and compared to each other. Both seals are installed at their respective sealing positions, and the corresponding frictional torques are measured. The experimental results, obtained when the shaft rotates at 300 rpm, are presented in Fig. 6. The results indicate that the frictional torque for the MRF seal is approximately 0.13 Nm, which is significantly smaller than the frictional torque of the lip-seal, which measures around 0.155 Nm. This observation highlights one of the advantages of MRF seals over lip-seals, as the MRF seal exhibits lower frictional torque. This outcome aligns with expectations and demonstrates the improved performance of the MRF seal in terms of reducing friction compared to traditional lip-seals.

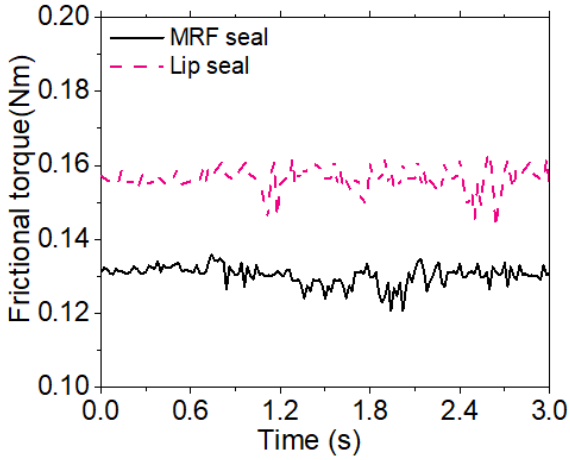

Fig. 6. Measured frictional torque of the MRF seal

In the second experiment, the maximum working pressure of the MRF seal is investigated. The experimental setup involves stopping the motor and connecting a cylinder-piston pressurized system to the pressure control port on the housing. The pressure is gradually increased in steps of 2.5 bar, and each pressure step is maintained for 1 minutes. The observation slot is used to monitor any leaking of the MRF. The experimental results, shown in Fig. 7, indicate that MRF leakage is observed when the pressure in the chamber reaches 25.5 bar. This value is slightly lower than the calculated maximum working pressure of 26.18 bar. The difference between the experimental and calculated values could be attributed to factors such as magnetic losses, inaccurate input of material properties,

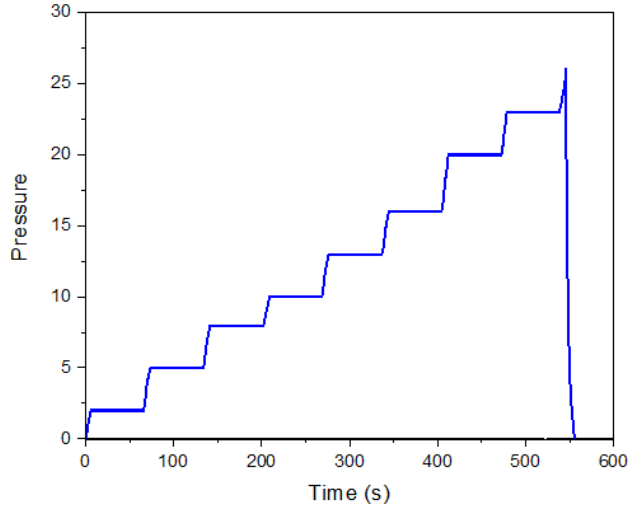

Fig. 7. Experiment results for step pressure increment for MRF seal

or manufacturing inaccuracies. It is worth noting that, in contrast to the MRF seal, the chamber pressure for lip-seals is typically limited to around 1 bar. This limitation arises due to factors like high frictional torque, heat generation, wear, and the overall lifespan of the lip-seal.

7. CONCLUSIONS

In this study, a novel magneto-rheological fluid (MRF) seal, referred to as the MRF seal, is proposed as a potential alternative to conventional lip-seals in MRF-based devices like MRB brakes, MR clutches, and MR actuators. The research begins with an overview of MR fluid and its applications, focusing on the state-of-the-art MRF-based seals. The configuration and working principle of the proposed MRF seal are then introduced. To design and model the MRF seal, the Bingham plastic rheological model of the MR fluid and finite element analysis are utilized. The design process incorporates finite element analysis using the first-order method integrated in ANSYS-Mechanical APDL. This analysis aids in obtaining an optimal design for the MRF seal. Based on the results of the finite element analysis, an optimal design of the MRF seal is achieved. Subsequently, two prototypes of the MRF seal are fabricated for experimental evaluation. Experimental tests specifically focusing on frictional torque reveal that the MRF seal exhibits significantly lower frictional torque compared to the lip seal. The measured frictional torques are 0.13 Nm and 0.155 Nm for the MRF seal and lip seal, respectively. The experimental investigation also assesses the maximum working pressure of the MRF prototype seals, which is found to be 25.5 bar. This value is close to the calculated working pressure of 26.18 bar and considerably higher than the working pressure of the equivalent lip-seal, which is limited to 1 bar. Future research endeavors will involve exploring different pole shapes, conducting multi-objective optimization, and performing additional experimental investigations on the MRF seals. These experiments will focus on factors such as the seal's lifetime in relation to shaft speed and working pressure.

ACKNOWLEDGEMENT

This work was supported by research fund from Ministry of Education and Training (MOET) of Vietnam under the grand no. B2022-VGU-03.

DECLARATION OF COMPETING INTEREST

The authors declare that they have no known competing financial interests or personal relationships that could have appeared to influence the work reported in this paper.

REFERENCES

[1] W. I. Kordonski and S. R. Gorodkin. Magnetorheological fluid-based seal. *Journal of Intelligent Material Systems and Structures*, **7**, (1996), pp. 569–572. https://doi.org/10.1177/1045389x9600700518.

[2] L. Matuszewski and Z. Szydło. The application of magnetic fluids in sealing nodes designed for operation in difficult conditions and in machines used in sea environment. *Polish Maritime Research*, **15**, (2008), pp. 49–58. https://doi.org/10.2478/v10012-007-0083-0.

[3] H. Urreta, G. Aguirre, P. Kuzhir, and L. N. L. de Lacalle. Seals based on magnetic fluids for high precision spindles of machine tools. *International Journal of Precision Engineering and Manufacturing*, **19**, (2018), pp. 495–503. https://doi.org/10.1007/s12541-018-0060-9.

[4] C. Hegger and J. Maas. Smart sealing for magnetorheological fluid actuators. *Journal of Intelligent Material Systems and Structures*, **30**, (2018), pp. 689–700. https://doi.org/10.1177/1045389x17754261.

[5] M. Kubík, D. Pavlíček, O. Macháček, Z. Strecker, and J. Roupec. A magnetorheological fluid shaft seal with low friction torque. *Smart Materials and Structures*, **28**, (2019). https://doi.org/10.1088/1361-665x/ab0834.

[6] Q.-H. Nguyen, Y.-M. Han, S.-B. Choi, and N. M. Wereley. Geometry optimization of MR valves constrained in a specific volume using the finite element method. *Smart Materials and Structures*, **16**, (2007), pp. 2242–2252. https://doi.org/10.1088/0964-1726/16/6/027.

[7] M. I. Varela-Jiménez, J. L. V. Luna, J. A. Cortés-Ramírez, and G. Song. Constitutive model for shear yield stress of magnetorheological fluid based on the concept of state transition. *Smart Materials and Structures*, **24**, (2015). https://doi.org/10.1088/0964-1726/24/4/045039.

[8] Q. H. Nguyen and S. B. Choi. Optimal design of a novel hybrid MR brake for motorcycles considering axial and radial magnetic flux. *Smart Materials and Structures*, **21**, (2012). https://doi.org/10.1088/0964-1726/21/5/055003.